Heat transfer in compact cross-flow mini heat exchanger

Mateusz Prończuk[*], **Aleksander Pabiś**

Department of Chemical Engineering and Technology, Tadeusz Kościuszko Cracow University of Technology, ul. Warszawska 24, 31-155 Kraków, Poland
[*]*Corresponding author: e-mail:* mateusz.pronczuk@pk.edu.pl

This paper presents the results of an analysis of heat transfer in a cross-flow mini heat exchanger (CFMHE). The purpose of the paper was to analyze the results of the experimental measurements presented in the previous work in order to determine dimensionless correlations that allow for the calculation of heat transfer coefficients for the CFMHE. Analyzed CFMHE consisted of a brass cylindrical core, in which 2 mm circular holes were drilled. A method based on an optimization procedure was used to determine the correlations describing the heat transfer coefficients, allowing the correlations to be determined without the need of measuring the mini channel wall temperature. Overall heat transfer coefficients calculated using the proposed correlations typically did not deviate by more than ±10% from the corresponding experimental results, which was a significant improvement in the quality of the fit compared to the results presented in previous work.

Keywords: heat transfer, cross-flow, mini heat exchanger, optimization based method.

INTRODUCTION

Miniaturization of devices and, in particular, heat and mass exchangers and reactors became possible thanks to inventions in electronics such as transistors and then integrated circuits and microprocessors. This enabled thousands or even millions of electronic components to be packed in a miniature silicon wafer with an area smaller than a fingernail. This was made possible through the use of microlithography, which involves sputtering thin films, exposing them and etching them with reactive chemicals to create electrical circuits on the surface of a silicon monocrystals. The techniques used in electronics, after some modifications, were also used in the construction of micro-devices and, in particular, micro-exchangers. The main problem to be solved was the formation of micro channels and the joining of very thin wafers in which they were made.

Currently, the most common methods used to create micro channels and form compact structures from machined wafers include[1]: micromachining, diffusion welding, stereolithography, chemical etching and X-ray treatment (limited ability for obtaining channel widths and depths up to a maximum of 10 μm). There are many different ways to classify channels based on their diameter available in the literature. Mehendale and co-workers[2] classified exchangers according to the hydraulic diameter of their channels into: micro heat exchangers ($D_h = 1 – 100$ μm), meso heat exchangers ($D_h = 100 – 1000$ μm), compact or mini heat exchangers ($D_h = 1 – 6$ mm) and conventional heat exchangers ($D_h > 6$ mm).

Initially, miniaturization in the construction of exchangers was mainly of interest to the space industry and the military in the United States. Later, there were opportunities to use miniature devices in other fields as well, due to their unquestionable advantages. These include: favorable ratio of heat transfer surface area to occupied volume; operation in most cases in the laminar range; very high heat transfer coefficients in the order of 10 – 35 kW/(m²K), using channels with hydraulic diameters of several to several hundred micrometers and ability to operate at high temperatures and pressures (for example, miniature heat exchangers from Heatric

Ltd[3] can operate at pressures up to 650 bar and in the temperature range from 4 to 1137 K).

The micro heat exchanger presented in the paper by Kang and co-authors[4] illustrates well the advantages mentioned above. It was made of 26 silicon wafers and has 1625 channels on the side for each medium, each channel being 40 μm wide and 200 μm deep. The total heat transfer area on one side is 70.2 cm² and the ratio of the area to the volume in which heat transfer occurs F/V = 15295 m²/m³. For the heat flux exchanged of $\dot{Q}$ = 5 kW an overall heat transfer coefficient of U = 24.7 kW/(m²K) was achieved.

The mini heat exchanger presented in this article admittedly does not match the performance of the micro heat exchanger described above due to the diameter of the channels $D_e = 2$ mm. The original study of heat transfer in the investigated cross flow mini heat exchanger was described in the previous work[5]. Its advantages are relatively low pressure loss, higher overall heat transfer coefficients compared to classic shell-and-tube heat exchangers, less possibility of deposition of any impurities and, if they occur, ease of mechanical cleaning. In addition to the basic measurements, some individual heat exchange tests were also carried out in the following systems: flue gas – cold water, steam – water, hot air – cold water. They confirmed the advantages of this heat exchanger.

This paper mainly focuses on the analysis of the results presented in an earlier paper[5]. That paper presented the results of overall heat transfer coefficient measurements for an exchanger operating in a water-water system. Experimental values of overall heat transfer coefficients were determined, and a simple model was proposed to calculate the overall heat transfer coefficient for the investigated heat exchanger as a function of flow rates and initial temperature of hot water. However, the proposed model has significant discrepancies between the experimentally determined overall heat transfer coefficient and the one calculated using that model, reaching up to several hundred percent in some cases.

The overall heat transfer coefficient can be determined with much better accuracy using dimensionless correlations that allow the calculation of heat transfer

coefficients for both fluids circulating in the exchangers. Such correlations are conventionally determined based on experimental measurements, during which, in addition to the temperature of the fluid flowing in the channel, the temperature of the wall of the channel must also be measured. The temperature difference between the wall and the fluid core is the driving force behind the convective heat transfer process, and it can be used (knowing the amount of exchanged heat and the heat transfer area) to determine the heat transfer coefficient. By conducting a series of such experiments, it is possible to determine dimensionless equations linking the exchanger's operating parameters, the physical properties of the fluid and the heat transfer coefficient. Unfortunately, for the heat exchanger under study, such an approach is not feasible, because the diameter of the smallest temperature sensors is comparable to that of the diameter of the channel, so such a sensor would significantly impede or even block the flow of the fluid.

A solution to this problem can be the use of an optimization procedure to determine correlations that combine the heat transfer coefficient (as a function of the dimensionless Nusselt number) with the dimensionless Reynolds and Prandtl numbers. Such an approach has been successfully applied to the determination of heat transfer coefficients in a shell and tube mini heat exchanger (STMHE), as described in detail in the previous paper by Prończuk and Krzanowska[6]. In this method, instead of determining the respective values of heat transfer coefficients, the form of the dimensionless correlation describing the coefficient is assumed, and then the values of the parameters of this equation are adjusted with optimization methods so that the overall heat transfer coefficient calculated using them deviates as little as possible from the value of the heat transfer coefficient determined by experiments (which can be performed knowing only the temperatures and flow rates of the process media). This work presents the results of applying the optimization method to the analysis of heat transfer in the aforementioned cross flow mini heat exchanger (CFMHE).

Experimental setup

The present work covers only the analysis of experimental results originally presented in a publication by Pabiś[5], photograph of the experimental setup and the schematic diagram of the test section are presented in the Fig. 1a-b, respectively. The aforementioned paper presented the results of the experimental determination of overall heat transfer coefficients for the cross flow mini heat exchanger (CFMHE) under study. This paper attempts to determine heat transfer coefficients for hot and cold media. The both of which were water. The hot water loop consisted $n_h = 22$ of channels of circular cross-section drilled into the brass core of the heat changer. The channels had a diameter of $D_h = 2$ mm and a length of $L_h = 30.5$ mm and were arranged in 4 rows, parallel to the axis of the cylindrical core. The cold water flow, on the other hand, consisted of $n_c = 18$ circular channels with a diameter and length of $D_c = 2$ mm and $L_c = 25.5$ mm, respectively, and two rectangular channels along the side of the cylindrical part with a height of $H_{rc} = 0.8$ mm, width $W_{rc} = 25.5$ mm and
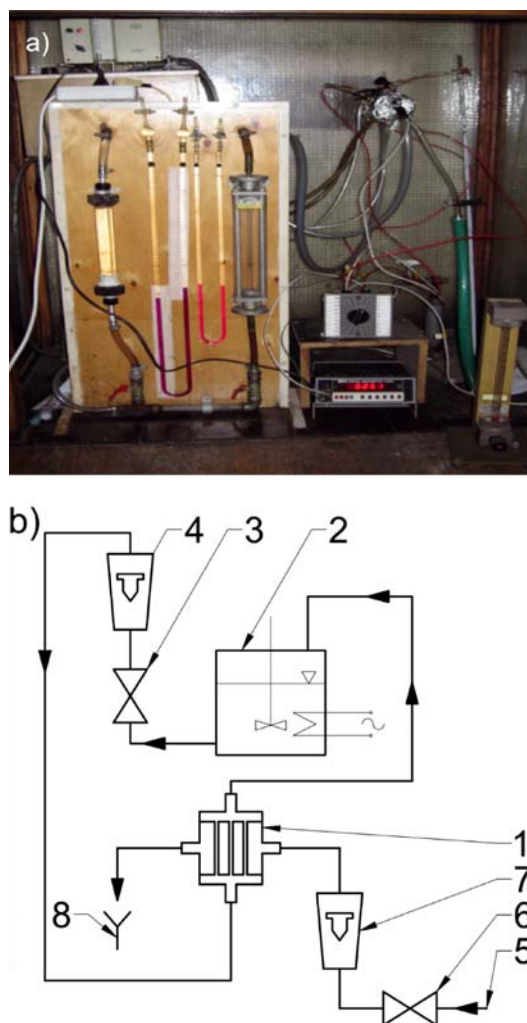

Figure 1. a) Picture of the test section, b) Schematic drawing of the test section: 1 – investigated heat exchanger, 2 – thermostatic vessel, 3 – hot water valve, 4 – hot water rotameter, 5 – cold water inlet, 6 – cold water valve, 7 – cold water rotameter, 8 – water drain

length $L_{rc} = 28.2$ mm. Drawing of the cross-section of the CFMHE under study is shown in Fig. 2. Hot water was heated using a thermostatic vessel and supplied to the exchanger with a flow rate $\dot{V}_h = 100 - 290 \ dm^3/h$ of and initial temperature in the range of $T_{ih} = 40 - 70$ºC. This resulted in the Reynolds number for the hot water loop in the range of $Re_h = 1200 - 3800$. Cold water was supplied directly from the water supply network with an volumetric flow rate in the range of $\dot{V}_c = 10 - 290 \ dm^3/h$ and the initial temperature of about $T_{ic} = 8$ºC. For the cold water loop, the Reynolds number values was in the range of $R_{ec} = 60 - 1440$. The amount of heat exchanged in the analyzed CFMHE was in the range of $Q = 110 - 1190$ W. The results of 1682 experiments were used to analyze the experimental results.

Materials

As mentioned earlier, both as a hot and cold medium, tap water was used. Measurements of thermal and physicochemical properties for tap water showed that they did not differ significantly from those of pure water (the measured differences were within the limits of measurement error). Thus, the physicochemical properties of pure water (density, viscosity, heat transfer coefficient and specific heat) taken from tables were adopted, and their
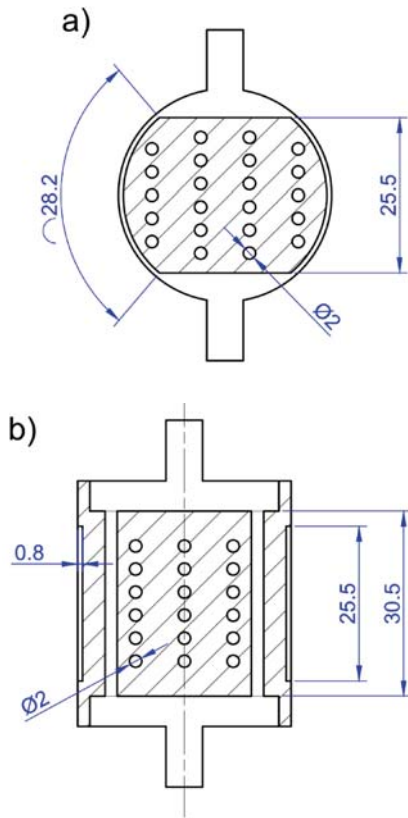
Figure 2. Drawings of the cross-sections of the analyzed CFM-HE: a) perpendicular to the hot water channels, b) perpendicular to the cold water channels

values for particular temperatures were approximated using polynomials. The core of the heat exchanger was made of brass. A constant value of thermal conductivity of brass equal to $k_w = 110$ W/(mK) was adopted for the calculations. The heat exchanger shell was made of copper, and a layer of mineral wool 20 mm thick was used for insulation of the heat exchanger.

Methodology

During the experiments, measurements of the initial and final temperatures in the cold water flow, the initial and final temperatures in the hot water flow, and the flow rates of hot water and cold water were carried out. The first step in determining the overall heat transfer coefficient was to determine the average temperature in each loop. The physical properties were calculated for the determined average temperature of the water in the given loop. Using the measured temperatures, flow rates and the determined physical properties, the amount of heat taken away by the cold water (1), $\dot{Q}_c$, and the amount of heat given off by the hot water (2), $\dot{Q}_h$ were calculated:

$$\dot{Q}_c = \dot{V}_c \rho_c c_{pc} (T_{fc} - T_{ic}) \tag{1}$$

$$\dot{Q}_h = \dot{V}_h \rho_h c_{ph} (T_{ih} - T_{fh}) \tag{2}$$

Where: $\dot{V}$ – volumetric flow rate, m³/s; ρ – water density, kg/m³; c_p – specific heat, J/(kg K); T_i, T_f, – initial and final temperature, ºC; c, h – indexes referring to cold or hot water.

The amount of heat transferred in the heat exchanger, $\dot{Q}$, was determined as the average of the amount of heat transferred by the hot water and received by the cold water (3):

$$\dot{Q} = \frac{\dot{Q}_c + \dot{Q}_h}{2} \tag{3}$$

The heat transfer surface area for the hot water loop, A_h, was determined based on the number of channels, their diameter and length (4). For the cold water circuit, the heat transfer surface area, A_c, was determined from the number of channels, their diameter and length, and from as well as the length and width of the two channels along the side of the cylindrical core (5):

$$A_h = \pi D_h n_h L_h = 0.004216 \, m^2 \tag{4}$$

$$A_c = \pi D_c n_c L_c + 2 W_{rc} L_{rc} = 0.004322 \, m^2 \tag{5}$$

Where: n – number of channels; D – channel diameter, m; L – circular channel length, m; L_r – rectangular channel length, m; W_{rc} – width of the rectangular channel, m.

The mean heat transfer area, A, was determined using the logarithmic mean (6):

$$A = \frac{A_h - A_c}{\ln \frac{A_h}{A_c}} = 0.004269 \, m^2 \tag{6}$$

The average driving force of the heat transfer process was determined using average logarithmic temperature difference, ΔT_m, as for the countercurrent flow (7):

$$\Delta T_m = \frac{(T_{ih} - T_{fc}) - (T_{fh} - T_{ic})}{\ln \frac{T_{ih} - T_{fc}}{T_{fh} - T_{ic}}} \tag{7}$$

Since the media flow in the heat exchanger was not strictly countercurrent flow but cross-flow, the overall heat transfer coefficient calculation had to take into account the cross-flow correction factor, F, which was determined based on the temperatures of the media in the heat exchanger and the tabulated values of this correction provided in the book by Hobler[7]. The minimum value of this correction of $F = 0.993$ indicates that the cross-flow caused only a slight reduction in the driving force of the process.

By knowing the heat transfer rate, $\dot{Q}$, heat transfer surface area, A, the average driving force of the process, ΔT_m, and the value of the correction to account for cross-flow of media, F, it was possible to determine the value of the overall heat transfer coefficient (8), U_{exp}:

$$U_{exp} = \frac{\dot{Q}}{A F \Delta T_m} \tag{8}$$

The experimentally determined overall heat transfer coefficients were used to determine the heat transfer coefficients for both water flows in the heat exchanger. To determine them, a method based on optimization was used, which was described in detail in a previous paper[6]. This method involves assuming the form of dimensionless equations that allow the determination of the values of heat transfer coefficients, followed by optimization-based adjustment of the parameter values for these equations. Such equations are often based on dimensionless Nusselt numbers, Nu, Reynolds numbers, Re, and Prandtl numbers, Pr. In this paper, the following forms of dimensionless equations were assumed for hot water flow (9) and cold water flow (10):

$$Nu_h = C_h \left(Re_h^{a_h} + d_h \right) Pr_h^{b_h} \tag{9}$$

$$Nu_c = C_c \left(Re_c^{a_c} + d_c \right) Pr_c^{b_c} \tag{10}$$

Where *a*, *b*, *C*, *d* are parameters of the proposed equations.

The forms of the equations were chosen to be similar to the most common forms of equations describing heat transfer. The Reynolds (11), Prandtl (12) and Nusselt (13) dimensionless numbers were defined as follows:

$$Re = \frac{u\rho D_e}{\mu} \tag{11}$$

$$Pr = \frac{c_p \mu}{k} \tag{12}$$

$$Nu = \frac{hD_e}{k} \tag{13}$$

Where: *h* – heat transfer coefficient, W/(m²K); D_e – equivalent diameter, m; *k* – heat conduction coefficient, W/(m K); *u* – mean flow velocity, m/s; *ρ* – liquid density, kg/m³; *μ* – dynamic viscosity coefficient, Pa s; c_p – specific heat, J/(kg K).

For the hot water loop, which consisted solely of circular channels, the equivalent diameter was equal to the diameter of the channel ($D_{eh} = D_h = 2$ mm). For the cold water circuit, due to the presence of rectangular channels along the side of the cylinder, the equivalent diameter, D_{ec}, was calculated as (14):

$$D_{ec} = \frac{4\left(\frac{\pi D_c^2}{4}n_c + 2W_{rc}H_{rc}\right)}{\pi D_c n_c + 2(2W_{rc} + 2H_{rc})} = 2.590\ mm \tag{14}$$

The calculated heat transfer coefficients can be used to calculate the overall heat transfer coefficient, U_{calc}, using the equation (15):

$$U_{calc} = \frac{1}{\frac{1}{h_c} + \frac{s}{k_w} + \frac{1}{h_h}} \tag{15}$$

Where is the thickness of the wall through which heat is conducted. In the CFMHE studied, the distance between the rows of the hot and cold flow loops was *s* = 2 mm.

The aim of this study was to determine the values of heat transfer coefficients by selecting the parameters of equations (9) and (10) in such a way that the differences between the experimentally determined and calculated heat transfer coefficients are minimized, so we can define the objective function as (16):

$$F = \sum_{i=1}^{n} \left(U_{calc,i} - U_{exp,i}\right)^2 \tag{16}$$

Thus, we can outlie the optimization algorithm as follows:

1. Experimentally determine the overall heat transfer coefficients (eqs. (1)–(8)).

2. Assume the form of the equations describing heat transfer (eqs. (9)–(10)).

3. Randomly select of the parameters of eqs. (9)–(10) from the assumed variability range.

4. Determine the dimensionless *Re*, *Pr* and *Nu* numbers using eqs. (9)–(12).

5. Calculate heat transfer coefficients using *Nu* number definition (13).

6. Calculate the overall heat transfer coefficient using equation (15).

7. Determine the value of the objective function (16) and adjust the parameters of equations (9) and (10) using the optimization procedure until the minimum of the objective function (16) is achieved.

Complex objective functions, especially those based on experimental data, may have several local minima. To find the global minimum of the objective function, the optimization procedure was repeated a hundred times, and the set of parameters of equations (9) and (10) that yielded the lowest value of the objective function was considered as the final result.

All calculations performed in this work were obtained using Matlab[8] version 2021b. To find the minimum of the objective function, the fmincon function was used, which allows for determining the minimum of the objective function with multiple variables and constraints of various types. Only the minimum and maximum bounds of the parameters of equations (9) and (10) were restricted in the optimization procedure. The optimized objective function had a total of up to eight variables, the values of which were selected by optimization. The calculations used default values of optimality tolerance (10⁻⁶) and step tolerance (10⁻¹⁰). Attempts were made to reduce these tolerances, however, they resulted in a significant increase in computation time without a noticeable improvement in the accuracy of the obtained solutions.

The numerical procedure employed enabled the derivation of correlations for calculating Nusselt number values based on Reynolds and Prandtl numbers, and subsequently, using the Nusselt number definition, heat transfer coefficients for both water flows. The obtained heat transfer coefficients were then compared with coefficients calculated using other correlations available in the literature. Thirteen correlations[9–17] derived for different flow regimes and for different channel types were selected for comparison (equations (17)–(29)). Among the selected correlations, seven of them[9–13] were developed for conventional channels (equations (17)–(23)), while the remaining six[14–17] were derived specifically for heat transfer in mini and micro channels (equations (24)–(29)).

For conventional channels, circular cross-section channels are the most common. However, in the case of heat transfer in mini and micro channels, often the cross-sectional shape of the channel differs from circular, such as rectangular or triangular. For the purpose of the comparison, it was decided to select the correlations specifically for circular cross-section channels. In the case of the hot water loop, this is fully justified, since in this loop there were only channels with a circular cross-section. In the case of the cold water loop, however, we have both circular cross-section channels and two rectangular channels along the side of the cylindrical core of the heat exchanger. Correlations for the rectangular channels were omitted, though, because they required the width and height of the rectangular channel, so that the presence of parallel circular cross-section channels would be omitted. Instead, it was decided to consider all types of channels together, and their dimension was expressed in terms of equivalent diameter. A summary of all the correlations used for comparison purposes, along with their authors and applicability ranges, are summarized in Table 1.

Table 1. Dimensionless correlations for the Nusselt number used for the comparison with the proposed dimensionless correlations

| Authors	Correlation		Applicability range
Shah[9]	$Nu = 1.953\left(RePr\dfrac{D}{L}\right)^{1/3}$	(17)	$Re < 2\,100$ $\left(RePr\dfrac{D}{L}\right) \geq 33.3$
Sieder & Tate[10]	$Nu = 1.86\left(RePr\dfrac{D}{L}\right)^{1/3}$	(18)	$Re < 2\,100$ $0.48 < Pr < 16\,700$
Sieder & Tate[10]	$Nu = 0.027Re^{0.8}Pr^{1/3}$	(19)	$Re \geq 10\,000$ $L/D \geq 10$
Dittus & Boelter[11]	$Nu = 0.023Re^{0.8}Pr^{0.4}$	(20)	$Re \geq 10\,000$ $0.6 \leq Pr \leq 160$ $L/D \geq 10$
Hausen[12]	$Nu = 0.116(Re^{2/3} - 125)Pr^{1/3}\left[1 + \left(\dfrac{D}{L}\right)^{2/3}\right]$	(21)	$2\,100 \leq Re \leq 1\cdot 10^4$
Gnielinski[13]	$Nu = 0.012(Re^{0.87} - 280)Pr^{0.4}$	(22)	$3\,000 \leq Re \leq 10^5$ $1.5 \leq Pr \leq 500$
Gnielinski[13]	$Nu = \dfrac{\left(\dfrac{f_D}{8}\right)(Re - 1000)Pr}{1 + 12.7\left(\dfrac{f_D}{8}\right)^{1/2}(Pr^{2/3} - 1)}$ $f_D = [0.79\ln(Re) - 1.64]^{-2}$	(23)	$2\,300 \leq Re \leq 5\cdot 10^6$ $0.5 \leq Pr \leq 2\,000$
Ünverdi et al.[14]	$Nu = 9.3\cdot 10^{-4}Re^{1.183}Pr^{1/3}$	(24)	$1\,900 \leq Re \leq 5\,100$
Ünverdi et al.[14]	$Nu = 0.43Re^{0.463}Pr^{1/3}$	(25)	$5\,100 \leq Re \leq 1\cdot 10^4$
Choi et al.[15]	$Nu = 9.72\cdot 10^{-4}Re^{1.17}Pr^{1/3}$	(26)	$Re < 2\,000$
Choi et al.[15]	$Nu = 3.82\cdot 10^{-6}Re^{1.96}Pr^{1/3}$	(27)	$2\,500 \leq Re \leq 2\cdot 10^4$
Yu et al.[16]	$Nu = 7.0\cdot 10^{-3}Re^{1.2}Pr^{0.2}$	(28)	$6\,000 \leq Re \leq 2\cdot 10^4$
Adams et al.[17]	$Nu = Nu_{Gn}\left[1 + 7.6\cdot 10^{-5}Re\left(1 - \dfrac{D}{1.164}\right)\right]$ Nu_{Gn} is calculated using Gnielinski eq. (23)	(29)	$3\,200 \leq Re \leq 2\cdot 10^4$

Uncertainty analysis

Temperature measurement was carried out using pre-calibrated T-type thermocouples. Analysis of the calibration curve determined the magnitude of the temperature measurement uncertainty equal to $\delta T = 0.19^{\circ}C$. Factory-calibrated rotameters were used to measure flow rates, for which the measurement uncertainty was defined by the manufacturer as $\pm 5\%$ of the measured flow rate value. When analyzing measurement uncertainties, the effect of temperature measurement uncertainties on the values of the determined physical properties was neglected, because with such small temperature measurement uncertainties, their value was at least an order of magnitude smaller than the other measurement uncertainties. Uncertainties for functions of multiple variables $f(x_1, x_2, ..., x_n)$ were propagated to subsequent results using a function that allows calculation of the best approximation of uncertainty for independent measurements (30):

$$\delta f(x_1, x_2, ..., x_n) = \sqrt{\sum_{i=1}^{n}\left(\frac{\partial f(x_1, x_2, ..., x_n)}{\partial x_i}\delta x_1\right)^2} \quad (30)$$

RESULTS AND DISCUSSION

To assess the accuracy of the determined results, uncertainties were determined for the overall heat transfer coefficients. The results are presented in Fig. 3. From the figure, it can be observed that approximately 9 out
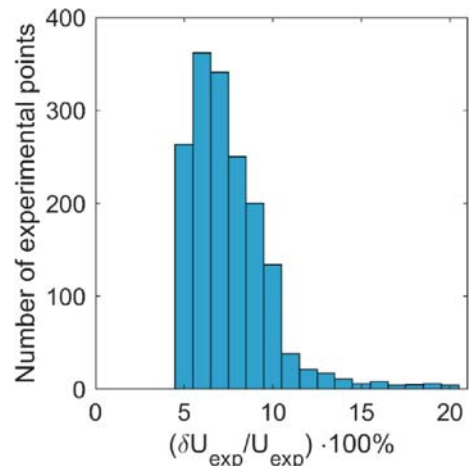
Figure 3. Histogram of the relative uncertainties of the overall heat transfer coefficient determined experimentally, U_{exp}

of 10 measurements carried out have a relative error of less than 10% (with a median 7.2%). It confirms the acceptable accuracy of the obtained results.

In order to determine the values of the parameters of equations (9) and (10) using optimization procedure, it was necessary to establish the boundary values of these parameters. The boundary values were selected based on other correlations of a similar type found in the literature. The boundary values of the coefficients are presented in Table 2.

Table 2. Lower and upper boundary values of the equations (9) and (10) parameters

Boundary value	a_h	b_h	C_h	d_h	a_c	b_c	C_c	d_c
Lower boundary	0	0	0	–1000	0	0	0	–1000
Upper boundary	2	2	2	1000	2	2	2	1000

Many types of dimensionless equations for determining heat transfer coefficients are available in the literature[7, 9–17]. To calculate the most suitable set of parameters for equations (9) and (10), four series of calculations were performed. In some cases, the values of the selected parameters of equations (9)–(10) were fixed instead of computed using optimization procedure. These cases will be designated with Roman numerals throughout the remainder of the article, and the assumptions for the calculations in each case were as follows:

Case I – all parameters of equations (9) and (10) were determined using the optimization procedure.

Case II – the value of the parameters b_h and b_c was set equal to 0.33, the remaining parameters were determined using optimization procedure.

Case III – the value of the parameters d_h and d_c was set equal to 0, the remaining parameters were determined using optimization procedure.

Case IV – the value of the parameters b_h and b_c was set equal to 0.33, the value of the parameters d_h and d_c was set equal to 0, the remaining parameters were determined using optimization procedure.

The values of the parameters b_h and b_c, i.e. exponents of the power of the Prandtl number, were set equal to 0.33 in cases II and IV. This choice was based on the frequent occurrence of these exponents with this value in the literature[9–10, 12, 14–15] (see equations (17)–(19), (21) and (24)–(27)), similar approach can be found in the other experimental studies[14–15]. In this study, unlike the value range of the Reynolds number, the Prandtl number values varied within a relatively narrow range (2.8–4.6 for the hot water and 5.6–10.6 for the cold water), so the effect of these parameters on the value of the heat transfer coefficient could not be sufficiently determined using optimization algorithm. On the other hand, the parameters d_h and d_c are found only in a few dimensionless equations describing heat transfer[12, 13], so omitting them from the calculations (setting their value equal to zero for cases III and IV) is justified, since only a few researchers have found it necessary to take these parameters into account.

The results of the calculations performed for the four series of calculations are presented in Table 3. Additionally, the goodness of fit between the determined models and the experimental results is illustrated in the graphs shown in Fig. 4. Along with the calculated

Table 3. Calculated coefficients of equations (9) and (10). RMSE – Root Mean Squared Error of calculated overall heat transfer coefficient, U_{calc}, compared to experimentally determined overall heat transfer coefficient, U_{exp}; * – coefficient was set to the specific value

Case	a_h	b_h	C_h	d_h	a_c	b_c	C_c	d_c	RMSE
	–	–	–	–	–	–	–	–	$\frac{W}{m^2 K}$
I	0.605	0.498	0.0603	−48.9	0.975	$3.03 \cdot 10^{-12}$	0.0938	−44.8	154.3
II	0.775	0.33*	0.0129	−436	1.23	0.33*	0.0106	−352	167.3
III	0.472	0.562	0.258	0*	0.692	$2.77 \cdot 10^{-12}$	0.486	0*	155.6
IV	0.419	0.33*	0.489	0*	0.718	0.33*	0.223	0*	174.7
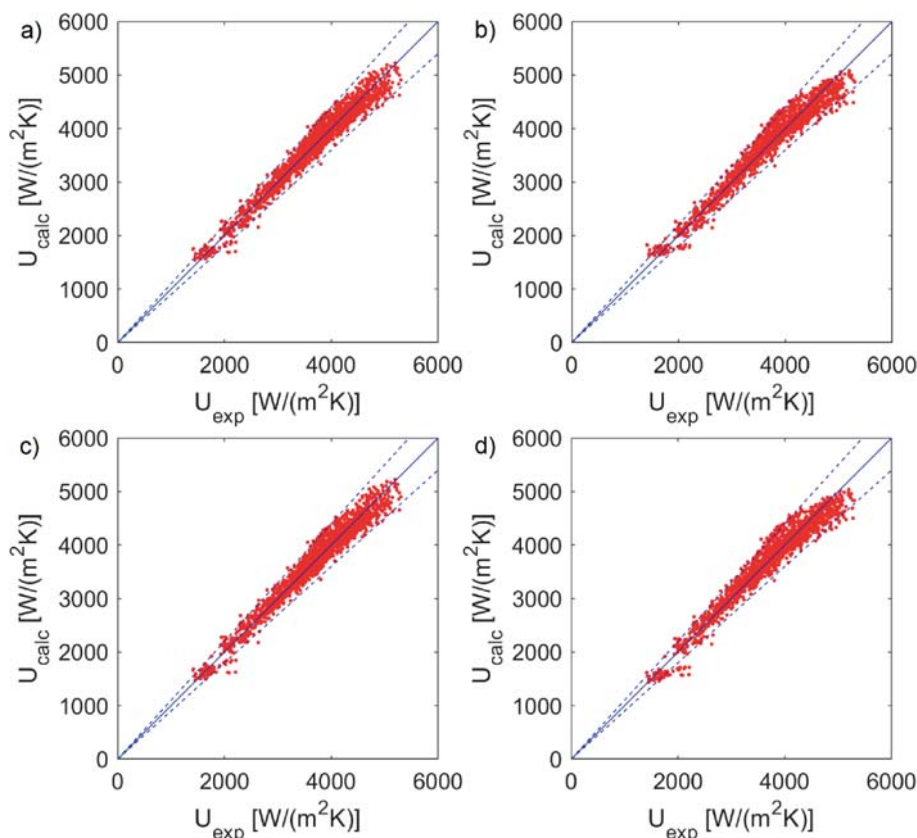
Figure 4. Comparison of experimentally determined overall heat transfer coefficient, U_{exp}, versus calculated values of overall heat transfer coefficient, U_{calc}, for the analyzed cases: a) I, b) II, c) III, d) IV. Solid blue line indicates $U_{exp} = U_{calc}$, dashed blue line indicates ±10% deviation

coefficients, the values of the root mean square error (RMSE) between the overall heat transfer coefficient values calculated using the optimization method and the overall heat transfer coefficient values determined experimentally were calculated using equation (31) and its values are provided in Table 3.

$$RMSE = \sqrt{\frac{1}{n} \sum_{i=1}^{n} \left(U_{exp} - U_{calc}\right)^2} \qquad (31)$$

When comparing cases I and II, it can be observed that setting the value of the exponent of the power of the Prandtl number to 0.33 results in a significant increase in the RMSE (from 154.3 W/(m²K) to 167.3 W/(m²K) for cases I and II, respectively), and thus indicating a deterioration in the model fit to the experimental data. However, it should be noted that the value of the exponent of the power of Prandtl's number in many different dimensionless correlations is most often equal to 0.33 (or 1/3). These correlations have often been derived for a variety of systems, by multiple different researchers, so this can be considered as generally accepted value. In the present study, only water was used as the medium, and the temperature range studied was relatively narrow, so that the value of the Prandtl number varied only within a narrow range. Therefore, despite the better fit of the correlation to the experimental results, a more correct approach is probably to assume the value of the exponent of the Prandtl number. Similar assumptions were also adopted by other researchers[14–15]. Additional confirmation of this assumption is provided by the calculated value of the exponent , which is very close to zero, which means that the heat transfer coefficient for the hot water circuit practically does not depend on the value of the Prandtl number, which contradicts reports available in the literature.

When comparing cases I and III, it can be observed that the quality of the fit, as determined by the RMSE, does not significantly depend on whether the coefficients d_h and d_c are included in the optimization procedure or whether their values are set to zero (the RMSE changes from 154.3 W/(m²K) to 155.6 W/(m²K) for cases I and III, respectively).

Setting the values of both the Prandtl number exponents b_h and b_c to 0.33 and the coefficients d_h and d_c to 0 (case IV) does not cause a significant change in the quality of the model fit to the experimental results compared to case II, where only the values of the Prandtl number exponents were assumed (RMSE changes from 167.3 W/(m₂K) to 174.7 W/(m²K) for cases II and IV, respectively).

However, it is important to note that despite the deterioration of the RMSE, the qualitative fit does not change significantly. Analyzing Fig. 4a-d, it can be observed that despite a significant increase in the RMSE, the qualitative fit remains relatively good, and most of the calculated overall heat transfer coefficients do not deviate by more than 10% from their experimentally determined values.

At this point, it is also necessary to refer to previous results obtained by analyzing the same experimental data, which were presented in the previous study[5]. The

aforementioned paper proposed a correlation based on the volumetric flow rates of hot water, $\dot{V}_h$ in dm³/h, cold water, $\dot{V}_c$ in dm³/h, and the initial temperature of hot water, T_{ih} in °C (32):

$$U_{calc} = 1480 + 7.42\dot{V}_c + 7.38\dot{V}_h + 1.52T_{ih} \qquad (32)$$

The overall heat transfer coefficients calculated using model (32) compared to the experimentally determined heat transfer coefficients are presented in Fig. 5. Upon analyzing the graph, significant discrepancies between the calculated and experimentally determined heat transfer coefficients can be observed, and a significant part of the calculated results have discrepancies much greater than ±10% (especially for the lower values of the heat transfer coefficient). The RMSE value for this model was much higher than for the models proposed in this paper, and was equal to 440 W/(m²K).
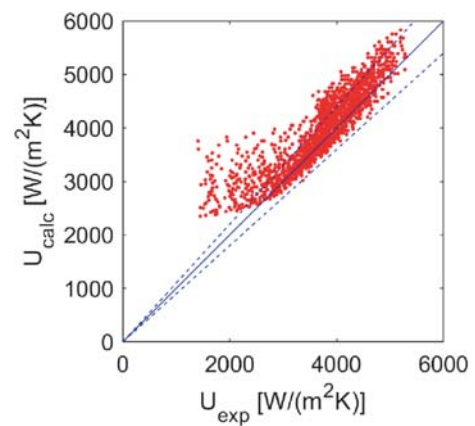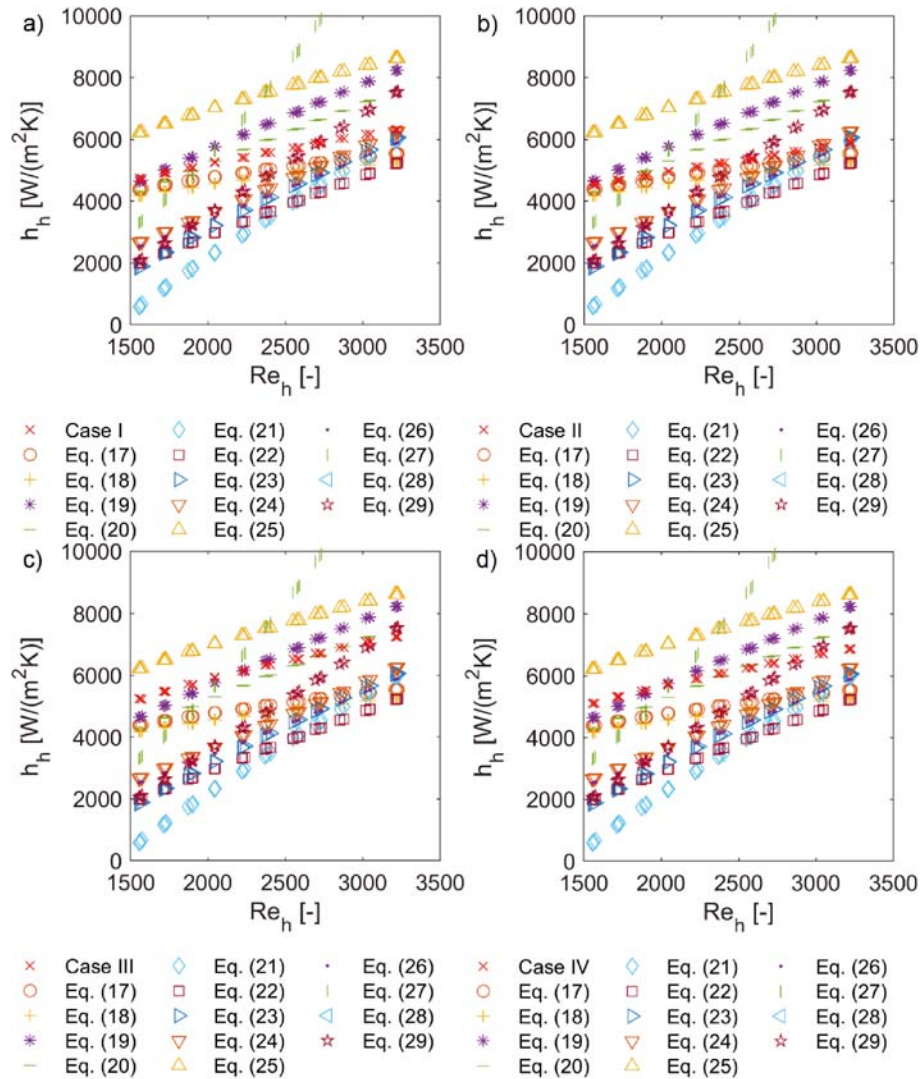
Figure 5. Comparison of experimentally determined overall heat transfer coefficient, U_{exp}, versus values of overall heat transfer coefficient calculated using correlation (19) from previous work[5]. Solid blue line indicates $U_{exp} = U_{calc}$, dashed blue line indicates ±10% deviation

Finally, other attempts were made to analyze the experimental results. An investigation were conducted whether, when increasing the flow rate of the media, the flow regime changes, and thus changes the form of the dimensionless correlation describing heat transfer coefficients. A similar analysis was previously successfully carried out for a shell-and-tube mini heat exchanger[6]. For this purpose, it was assumed that for both the hot water loop and the cold water loop, we can distinguish two different correlations to be used for a different range of Reynolds number values. To this end, the optimization procedure was extended to include a second set of dimensionless correlations of the form of equations (9) and (10), as well as critical values of the Reynolds number, representing the boundary between laminar and turbulent fluid flow in the given loop. Unfortunately, the critical Reynolds number values determined through optimization procedure always fell outside the experimental range of Reynolds number variability for a given loop, so no change in the fluid flow regime was found within the analyzed range of variability of heat exchanger operating parameters. Thus, the results obtained for the optimization procedure considering laminar and turbulent flow were then reduced to the results obtained for the procedure that did not consider the change in the flow regime.

The results of comparing the heat transfer coefficients calculated using the obtained correlations and correlations selected from the literature are presented in Fig. 6, for the hot water loop, and Fig. 7, for the cold water loop. The graphs illustrate the dependence of the calculated heat transfer coefficients as a function of Reynolds number. To accommodate multiple data series on a single graph, the results are shown for only one selected initial temperature of the hot water ($T_{ih} = 60°C$), and for every tenth measurement point. In addition to the qualitative comparison, the RMSE between heat transfer coefficients calculated using the chosen literature correlations and all four analyzed cases for the entire measurement data set (1682 measurements). The results for the hot water loop and for the cold water loop are shown in Table 4.

One notable observation is that the correlations obtained using the optimization procedure do not completely agree with each other for the different analyzed cases, depending on the adopted simplifications of the objective function being sought. These differences are not as
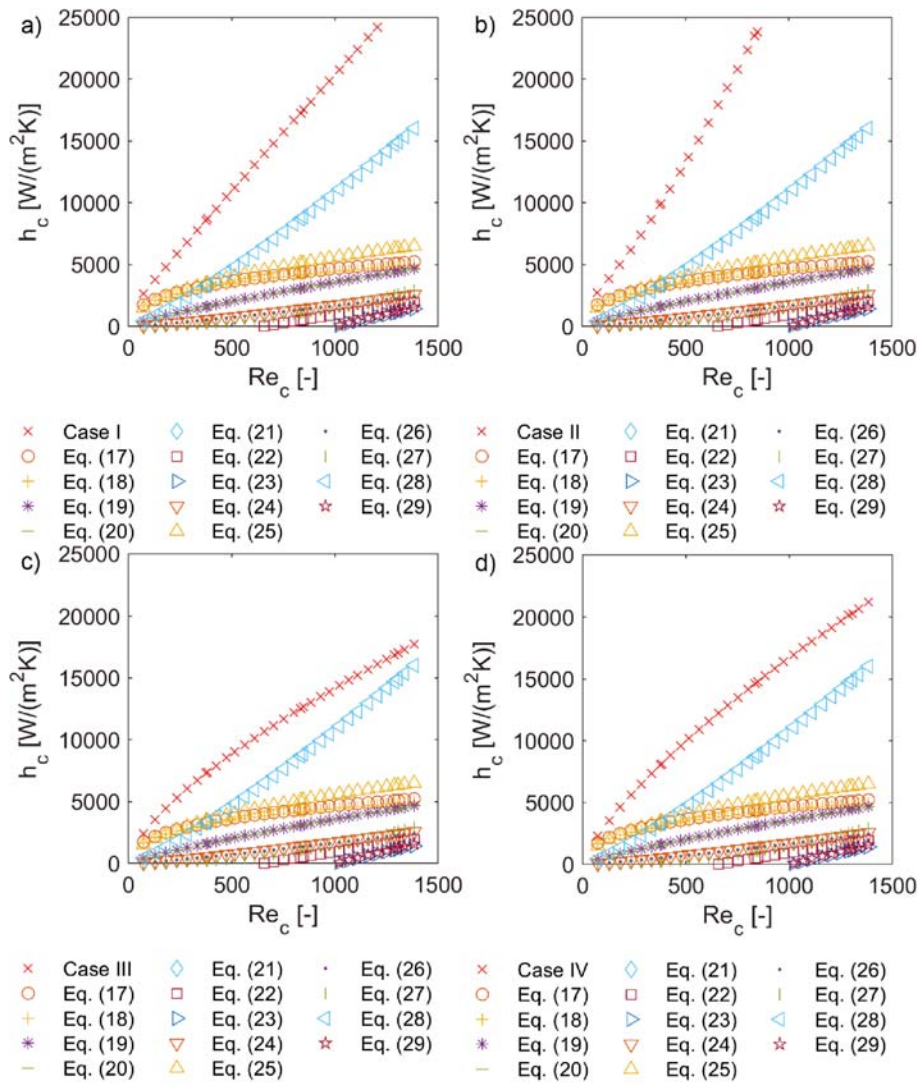

Figure 6. Comparison of experimentally determined heat transfer coefficient for the hot water loop, h_h, and its values calculated using correlations from the literature (equations (17)–(29)) versus hot water Reynolds number, Re_h, for the analyzed cases: a) I, b) II, c) III, d) IV

Table 4. Root mean squared error (RMSE) between heat transfer coefficients calculated using correlations from the literature (equations (17)–(29)) and correlations obtained using the optimization method (Cases I–IV). The best result for each case has been bolded

Equation number	Hot water RMSE [$W/(m^2K)$]				Cold water RMSE [$W/(m^2K)$]			
	Case I	Case II	Case III	Case IV	Case I	Case II	Case III	Case IV
(17)	**775**	**252**	1634	1106	13019	20408	7874	9975
(18)	996	496	1877	1351	13207	20591	8064	10165
(19)	1194	1616	**674**	888	14005	21328	8931	1109
(20)	801	1172	716	**625**	140024	21347	8951	11029
(21)	2751	2422	3426	3017	19405	26432	14616	16590
(22)	2146	1735	2940	2471	16371	23617	11368	13423
(23)	1966	1641	2666	2238	17726	24808	12905	14883
(24)	1472	1165	2184	1745	15548	22848	10488	12564
(25)	1902	2381	1053	1525	12291	19676	7154	9251
(26)	1653	1286	2413	1953	15613	22914	10551	12627
(27)	4532	4904	3913	4261	15676	22956	10637	12706
(28)	29635	30111	28771	29265	**8038**	**15254**	**3415**	**5246**
(29)	1757	1685	2160	1882	17730	24805	12919	14893

Figure 7. Comparison of experimentally determined heat transfer coefficient for the cold water loop, h_c, and its values calculated using correlations from the literature (equations (17)–(29)) versus cold water Reynolds number, Re_c, for the analyzed cases: a) I, b) II, c) III, d) IV

pronounced for the case of the hot water loop (Fig. 6), but in the case of the cold water loop they become significant (Fig. 7). Analyzing the discrepancies between the functions obtained through optimization and the results obtained using literature correlations (expressed using RMSE, see Table 4.), we can conclude that the best fit, depending on the case analyzed, for the hot water loop has correlations (17)–(20)[9–11] intended for the description of heat transfer in conventional channels. On the other hand, for the cold water loop, the best fit corresponds to correlation (28)[16] proposed for heat transfer in mini channels. However, it should be noted that none of the mentioned correlations adequately reproduces the correlations obtained using the optimization method.

CONCLUSIONS

The analysis of the experimental results of heat transfer in the cross flow mini heat exchanger has led to determination of correlations that enable the calculation of heat transfer coefficients for both flows of the CFMHE, as well as the overall heat transfer coefficient. The utilization of the optimization method has significantly enhanced the accuracy of determining the overall heat transfer coefficient compared to the previous work[5].

The optimization-based method provides flexibility in selecting the form of dimensionless equations that describe the convective heat transport. However, when analyzing the data, it is important to ensure that the range of variation of the operating parameters of the heat exchanger under analysis is sufficiently wide. Introducing overly complex equations with a narrow range of operating parameters values can lead to correlations that appear to have a better fit to experimental data, but may not generalize well to a broader range of operating parameters. Such a situation was also encountered in the present work, where the values of the exponents of the Prandtl number significantly deviated from those generally accepted in other scientific works (0.33 or 0.40). This deviation was likely due to the limited range of variability of Prandtl number. To further validate the obtained results, it would be advisable to extend the measurements to other process media and to increase the range of variability of such heat exchanger operating parameters as flow rates or initial temperatures of the media.

Unfortunately, the comparison of the correlations obtained in this study with those available in the literature was not successful. It was challenging to determine which of the selected correlations for comparison would

best represent heat transfer in the CFMHE under study. Several factors could have contributed to the discrepancy. Firstly, the relatively small length of the heat exchanger channels compared to their diameter might have hindered the full development of velocity profiles due to inlet effects. Secondly, the presence of small chambers dividing and combining the streams flowing through the various channels may have caused uneven distribution of the fluid within the CFMHE under study. And thirdly, the unique design of the cold water loop, combining two different types of channels, was not found in similar heat exchanger designs documented in the literature.

However, the notable advantage of the optimization method used in this work is that it eliminates the need to know the temperature of the inner wall of the heat exchanger. The conventional method of determining heat transfer coefficients relies on the measurement of this temperature, since it is the temperature difference between the wall and the fluid core that drives the convective heat transfer process. By using the optimization procedure, it is possible to bypass the need for direct measurement of this temperature, which would be impractical or impossible to achieve in apparatuses with such small channel diameters. The optimization method provides a viable approach for the analysis of heat transfer in the small form factor heat exchangers where direct measurement of the temperature of the inner wall is not feasible.

LITERATURE CITED

1. Kandlikar, S.G., & Grande, W.J. (2003). Evolution of microchannel flow passages--thermohydraulic performance and fabrication technology. *Heat Transfer Engin*., 24(1), 3–17. DOI: 10.1080/01457630304040.

2. Mehendale, S.S., Jacobi, A.M., & Shah, R.K. (2000). Fluid flow and heat transfer at micro-and meso-scales with application to heat exchanger design. *Appl. Mech. Rev*., vol. 53, no 7. DOI: 10.1115/1.3097347.

3. Heatric Ltd. Heatric Printed Circuit Heat Exchangers. Retrieved April 26, 2023, from https://www.heatric.com/heat-exchangers/

4. Kang, S.W., Chen, Y.T., & Chang, G.S. (2002). The manufacture and test of (110) orientated silicon based micro heat exchanger. *J. Appl. Sci. Engin*., 5(3), 129–136. DOI: 10.6180/jase.2002.5.3.02.

5. Pabiś, A. (2011). Charakterystyka pracy krzyżowo-prądowego mikrowymiennika ciepła. Chemik 2011, 65, 10, 983–990.

6. Prończuk, M., & Krzanowska, A. (2021). Experimental investigation of the heat transfer and pressure drop inside tubes and the shell of a minichannel shell and tube type heat exchanger. *Energies*, 14(24), 8563. DOI: 10.3390/en14248563.

7. Hobler, T. (1979). Ruch ciepła i wymienniki (wydanie V). Warszawa, Polska: Wydawnictwa Naukowo Techniczne.

8. The MathWorks, Inc. Matlab. Retrieved April 26, 2023, from https://www.mathworks.com/products/matlab.html

9. Shah, R.K. (1975). Thermal entry length solutions for the circular tube and parallel plates. In Proceedings of 3rd national heat and mass transfer conference 1975, Vol. 1, pp. 11–75. Indian Institute of Technology Bombay.

10. Sieder, E.N., & Tate, G.E. (1936). Heat transfer and pressure drop of liquids in tubes. *Ind. & Engin. Chem*., 28(12), 1429–1435. DOI: 10.1021/ie50324a027.

11. Dittus, F.W. (1930). Heat transfer in automobile radiators of the tube type. Univ. Calif. Pubs. Eng., 2, 443.

12. Hausen, H. (1959). New equations for heat transfer with free or forced flow [in German]. Allg. Waermetech, 9, 75–79.

13. Gnielinski, V. (1976). New equations for heat and mass transfer in turbulent pipe and channel flow. *Int. Chem. Eng*., 16(2), 359–368.

14. Ünverdi, M., Kücük, H., & Yılmaz, M.S. (2019). Experimental investigation of heat transfer and pressure drop in a mini-channel shell and tube heat exchanger. *J. Heat Mass Transfer,* 55, 1271–1286. DOI: 10.1007/s00231-018-2514-0.

15. Choi, S.B., Barron, R.F. & Warrington, R.O. (1991). Fluid flow and heat transfer in microtubes, in: Micromechanical Sensors, Actuators and Systems, ASME DSC, vol. 32, Atlanta, GA, pp. 123–134

16. Yu, D., Warrington, R.O., Barron, R. & Ameel, T. (1995). An experimental and theoretical investigation of fluid flow and heat transfer in microtubes, in: Proceedings of ASME/JSME Thermal Engineering Joint Conf., Maui, HI, pp. 523–530.

17. Adams, T.M., Abdel-Khalik, S.I., Jeter, S.M. & Qureshi, Z.H. (1998). An Experimental investigation of single-phase forced convection in microchannels, Internat. *J. Heat Mass Transfer*, 41, 851–857. DOI: 10.1016/S0017-9310(97)00180-4.